I&EC research
Industrial & Engineering Chemistry Research

pubs.acs.org/IECR

Article

Modeling and Control of COVID-19 Transmission from a Perspective of Polymerization Reaction Dynamics

Chijin Zhang, Zuwei Liao,* Jingyuan Sun, Yao Yang, Jingdai Wang, and Yongrong Yang

Cite This: *Ind. Eng. Chem. Res.* 2021, 60, 17650−17662

Read Online

ACCESS | Metrics & More | Article Recommendations | Supporting Information

ABSTRACT: Due to the serious economic losses and deaths caused by COVID-19, the modeling and control of such a pandemic has become a hot research topic. This paper finds an analogy between a polymerization reaction and COVID-19 transmission dynamics, which will provide a novel perspective to optimal control measures. Susceptible individuals, exposed people, infected cases, recovered population, and the dead can be assumed to be specific molecules in the polymerization system. In this paper, a hypothetical polymerization reactor is constructed to describe the transmission of an epidemic, and its kinetic parameters are regressed by the least-squares method. The intensity of social distancing u is considered to the mixing degree of the reaction system, and contact tracing and isolation ρ can be regarded as an external circulation in the main reactor to reduce the concentration of active species. Through these analogies, this model can predict the peak infection, deaths, and end time of the epidemic under different control measures to support the decision-making process. Without any measures (u = 1.0 and ρ = 0), more than 90% of the population would be infected. It takes several years to complete herd immunity by nonpharmacological intervention when the proportion of deaths is limited to less than 5%. However, vaccination can reduce the time to tens to hundreds of days, which is related to the maximum number of vaccines per day.

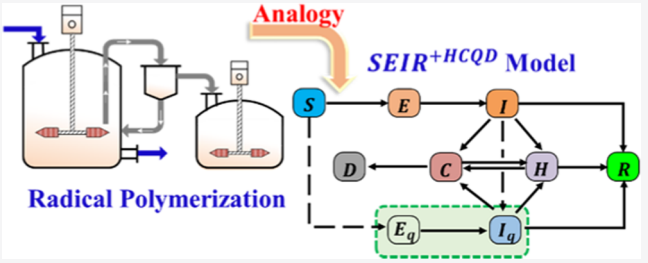

1. INTRODUCTION

A novel coronavirus termed as COVID-19 first broke out in Wuhan, Hubei Province, China, in December 2019, and it is observed that efficient human-to-human transmission of COVID-19 exists.[1] The World Health Organization (WHO) declared it a global pandemic and public health emergency on March 11, 2020.[2] More than 184 million individuals were infected and 3.99 million people died because of the virus as of July 5, 2021. Numerous measures and health system responses to this pandemic have been implemented at the national level. Wearing mask, staying at home, social distancing, contact tracing, and effective treatment are the important measures for epidemic mitigation and suppression.[3]

Mathematical models investigated to study COVID-19 generally consist of forecasting models and mechanistic models.[4] Forecasting models are usually used for statistical properties, fitting a line or curve, and predicting the future. Ribeiro et al.[5] collected epidemiologic data from the past in different states of Brazil and predicted the trend of COVID-19 by a stochastic-based regression model. Chakraborty and Ghosh[6] used a hybrid ARIMA-WBF model (autoregressive integrated moving average model and wavelet-based forecasting model) to simulate COVID-19 in various countries around the world. However, these forecasting models are not suited for long-term predictions about epidemiologic dynamics such as when the peak will occur and how effective various interventions will be. Mechanistic models such as the susceptible−exposed−infectious−recovered (SEIR) compartment model are utilized to describe future transmission scenarios under different assumptions. The epidemiological parameters changing with the implementation of control measures drive it to explore possible long-term epidemiologic outcomes. Wu et al.[7] used the SEIR model to simulate the epidemic in Wuhan and calculate the basic reproduction number R_0 = 2.68 based on the data reported from December 31, 2019 to January 28, 2020. R_0 is a measure for estimating the number of cases on average coming from the same infected case. In other reported studies,[8,9] the value of R_0 ranges from 2.0 to 4.7 due to the differences in COVID-19 control measures in different regions. Khajanchi et al.[8] proposed an extended $SARII_qS_q$ model and demonstrate that the elimination of ongoing COVID-19 is possible by combining the restrictive social distancing and contact tracing. Liu et al.[10] proposed a model that incorporates a time delay in infected persons before transmission is possible and evaluate the role of latency period in the dynamics of a COVID-19 epidemic. Peng

Received: September 9, 2021
Revised: November 11, 2021
Accepted: November 11, 2021
Published: November 22, 2021

https://doi.org/10.1021/acs.iecr.1c03647
Ind. Eng. Chem. Res. 2021, 60, 17650−17662

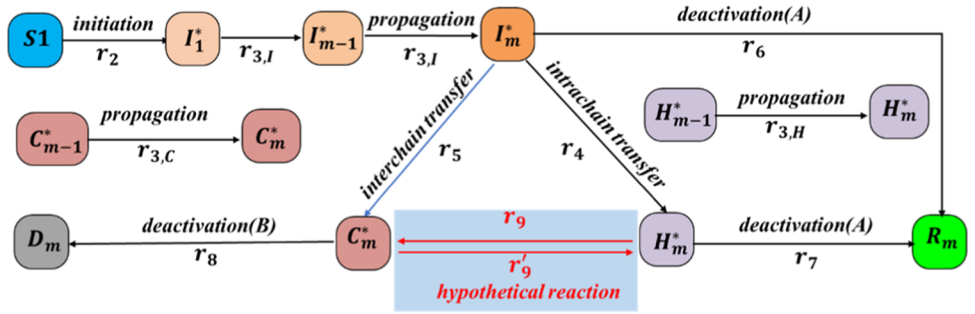

Figure 1. Polymerization reaction network for simulating the dynamics of COVID-19.

et al.[11] introduced three new compartments including insusceptible, quarantined, and dead individuals based on the SEIR model. The modified model is used to analyze the dynamic process of epidemics in various Chinese cities and estimate several key parameters for COVID-19 (like the latent time, quarantine time, and R_0).

Before the emergence of vaccines, the main control measures for preventing epidemic transmission are non-pharmaceutical interventions (NPIs).[12] Although several measures such as social distancing, stay-at-home order, and isolation can decrease the spread of the disease, they will reduce the economic output since the activities of people are also restricted. On the other hand, the capacity of the medical system is limited to treat the large inflow of potential patients who increase exponentially if there is no intervention.[13] Once the capacity of the medical system is overloaded, the mortality ratio of infected persons who have not received timely treatment may increase by two times.[14] Therefore, a tradeoff between the cost of NPIs and the number of deaths should be considered by policy makers. This problem is similar to the control optimization in the traditional chemical engineering field. In the chemical engineering production process, it is essential to ensure the stability of the entire system and avoid accidents caused by violent reactions. Meanwhile, we need to maximize production benefits by adjusting the operating conditions. An analogy between the epidemic model and the chemical reactor model is feasible under similar dynamics and optimization goals. Compared with epidemiology, dynamic optimization theory in chemical and biochemical engineering has a long and consolidated history.[15] Manenti et al.[16] proposed an analogy between the simple SIRD model and the behavior of chemical reactors by assuming each compartment to be molecules of chemical compounds. The corresponding predictive model based on chemical and physical considerations has been validated with data from different regions, which already underwent complete infection dynamics. Willis et al.[17] considered the effective regeneration number as the stoichiometric coefficient of the reactants and used the temperature to represent the intensity of the NPIs, and successfully developed a novel extension to the analogy between chemical and epidemiological system models. In the various chemical engineering reaction systems, the concentration of active chains in free-radical polymerization shows a similar S-shaped growth trend to those infected during the spread of epidemics. Meanwhile, limiting the concentration of active chains to prevent reactor explosions and controlling the number of infected persons to avoid large-scale spread of epidemics are very similar goals in different fields. Therefore, this provides a new method to study the control of epidemics from the perspective of the polymerization process.

The main works of this paper include to develop a new mathematical model that can describe the transmission dynamics and forecasting of COVID-19 in different regions and contribute to obtain the optimal control measures. Social distancing and contact tracing are two of the NPIs considered in this work, whose intensities are represented by variables $u(t)$ and $\rho(t)$, respectively. A hypothetical reactor is constructed for epidemic dynamics to "react" and a clear optimization process can be shown in this paper. The paper is organized as follows: In Section 2, it introduces a polymerization system with corresponding reaction dynamics to describe the transmission of COVID-19. Section 3 uses the least-squares algorithm to estimate the epidemiological parameters of the model in different regions. In Section 4, it conducts some model simulations to study the basic characteristics of the epidemic under different NPIs and construct the optimization model to obtain the optimized control measures with or without vaccines. Finally, a discussion in Section 5 concludes the paper.

2. MATHEMATICAL MODEL ANALOGY

The chemical reactor model consists of reactions and balances. Reactions determine the chemical transformations of molecules through kinetic mechanisms, while mass and energy balances give the nature and morphology of the reactor where transformations take place.[17] A bulk polymerization system with the free-radical polymerization mechanism is used to simulate the transmission of COVID-19. The reaction network is shown in Figure 1. People in different states can be considered as different chemical reactants and a reactor represents a specific region or country. Table 1 shows the meaning of each model parameter in the polymerization process and their corresponding meaning in the spread of an

Table 1. Analogy between the Polymerization Process and the Epidemic Spreading Process

parameter symbol	polymerization	epidemic
S	monomers for activation $S1$ and chain extension $S2$	susceptible population
I_m^*	basic active chain	infected people
H_m^*	active chain after intrachain transfer	hospitalized infected patients
C_m^*	active chain after interchain transfer	critical infected patients
R_m^*	dead polymer from A	recovered people
D_m^*	dead polymer from B	dead people
E^*	intermediate in monomer activation	exposed people

https://doi.org/10.1021/acs.iecr.1c03647
Ind. Eng. Chem. Res. 2021, 60, 17650−17662

Table 2. Reaction Equation and Rate in a Hypothetical Reactor

item	reaction equation	reaction rate
initiator cleavage	$\Theta \rightarrow 2\vartheta^*$ (1)	extremely fast
initiation	$S1 + \vartheta^* \rightarrow E^*$	$r_{2,\theta} = k_{i,\vartheta^*}[S1][\vartheta^*]$
	$S1 + I_m^* \rightarrow E^* + I_m^*$ (2)	$r_{2m,I} = k_{im,I_m^*}[S1][I_m^*]$ (11)
propagation	$S2 + F_m^* \rightarrow F_{m+1}^*$ (3)	$r_{(3m,F)} = k_{(pm,F)}[S2][F_m^*]$ (12)
intrachain transfer	$I_m^* \rightarrow H_m^*$ (4)	$r_{4m} = \alpha\beta k_{tm}[I_m^*]$ (13)
interchain transfer	$I_m^* \rightarrow C_m^*$ (5)	$r_{5m} = \alpha(1-\beta)k_{tm}[I_m^*]$ (14)
	$I_m^* \rightarrow R_m + \vartheta_d$ (6)	$r_{6m} = (1-\alpha)k_{tm}[I_m^*][A]$ (15)
deactivation	$H_m^* \rightarrow R_m + \vartheta_d$ (7)	$r_{7m} = (1-\gamma)k_{rm}[H_m^*][A]$ (16)
	$C_m^* \rightarrow D_m + \vartheta_d$ (8)	$r_{8m} = dk_{dm}[C_m^*][B]$ (17)
hypothetical	$H_m^* \leftrightharpoons C_m^*$ (9)	$r_{9m} = \gamma k_{rm}[H_m^*]$ $r'_{9m} = (1-d)k_{dm}[C_m^*]$ (18)
intermediate	$E^* \rightarrow I_1^*$ (10)	$r_E = \varphi[E^*]$ (19)

$F_m^* = \{I_m^*, H_m^*, C_m^*\}$, $G_m = \{R_m, D_m\}$, $\forall\, m \geq 1$
$k_{im,Im}^* = k_{i,Im}^*$, $k_{pm,F} = k_{p,F}$, $k_{tm} = k_t$, $k_{rm} = k_r$, $k_{dm} = k_d$, $\forall\, m \geq 1$

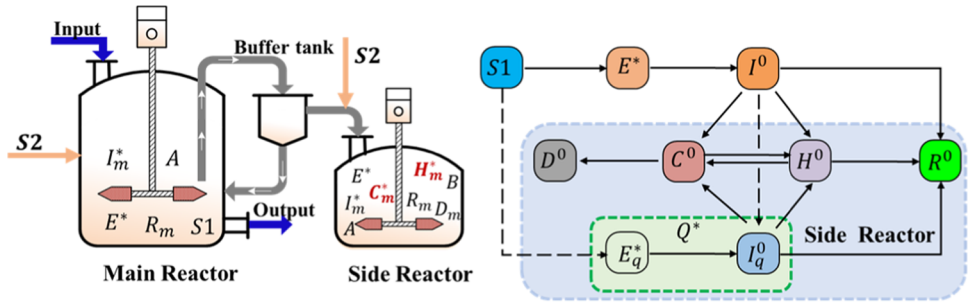

Figure 2. Reactor model and SEIR^{+HCQD} model.

epidemic context. In addition to the four basic compartments of the SEIR model, another three compartments are considered in our epidemic model, namely, hospitalized infected patients (H), critical infected patients (C), and dead people (D). Critical infected people need to use the intensive care unit (ICU) in which respiratory support or extracorporeal membrane oxygenation is supplied for the treatment; otherwise, there will be a higher possibility of death.[18]

First, monomer S is defined to represent susceptible people, while people infected for m days are realized as active chain free radicals I_m^* whose chain length is also m. The new coronavirus is like an initiator Θ that initiates monomers to form monomer free radicals I_1^*. Meanwhile, we assume that I_m^* can also activate monomers to generate I_1^*. The related reaction mechanism can be described as the chain initiation reaction 2 and intermediate reaction 10 in which the exposed individuals are regarded as intermediates E^* and the transition period is $1/\varphi$. According to the different consumption modes of the monomer, it is further divided into $S1$ and $S2$, and the former only generates I_1^*, while the latter is used to increase the chain length. Second, $\alpha(0 < \alpha < 1)$ portion of I_m^* would produce another two active chain free radicals H_m^* and C_m^* according to site transferring reactions 4 and 55, where the generation ratios of H_m^* and C_m^* are $\beta(0 < \beta < 1)$ and $1-\beta$, respectively. In addition, a hypothetical reversible reaction of r_9 and r'_9 is proposed between H_m^* and C_m^*. γ portion of H_m^* would turn into C_m^* and the rest $1-\gamma$ portion of H_m^* reacts with polymerization inhibitor A to form dead polymers R_m. Similarly, the d portion of C_m^* would lose activity and become dead polymers D_m when contacted with the polymerization inhibitor B, and the other C_m^* may produce H_m^* again. Finally, all active chain free radicals can react with monomer $S2$ for chain propagation (eq 3). H_m^* and C_m^* represent hospitalized infected patients and critical infected patients, and the dead polymers D_m and R_m represent dead people and recovered people, respectively.

Each reaction step is represented by a kinetic equation in a modified Arrhenius-type law where the temperature dependence is considered negligible due to the isothermal nature of the infection outbreak.[19] The chemical reactions are considered as first-order reactions, where the reaction rates are proportional to the reactant concentration. The chemical reaction rate expressions are stated in Table 2.

When dealing with radical polymerization kinetics, an equal activity assumption is made in which the activity of chain radicals is independent of the chain length m. Therefore, the rate constants of each elementary reaction are equal such as $k_{p1,F} = k_{p2,F} = k_{p3,F} = \cdots = k_{pm,F} = k_{p,F}$. Obviously, reaction rates (eqs 11−18) contain large number of equations and cannot be solved directly as the chain length m theoretically ranges from one to infinity. The moment model,[20,21] which defines the zero-order, first-order, and second-order moments (recorded by n) of the active chains F_m^* and dead polymer G_m as shown in eq 20, is used to transform the infinite-dimensional reaction

https://doi.org/10.1021/acs.iecr.1c03647
Ind. Eng. Chem. Res. 2021, 60, 17650−17662

equation system into a finite-dimensional equation system. Note that the concentrations of F^0 and G^0 have a specific relationship with the number of people in the corresponding compartments. The concentrations of inhibitors A and B are constants decided by hand

$$\begin{cases} F^n = \sum_{m=1}^{\infty} m^n [F_m^*] \\ G^n = \sum_{m=1}^{\infty} m^n [G_m] \end{cases}, \ n = 0, 1, 2 \tag{20}$$

Based on the above polymerization reaction network and a series of assumptions, the transmission process of COVID-19 under several control measures (use of face mask, social distancing, personal hygiene, contact tracing isolation, etc.) can be simulated in a hypothetical reactor. As shown in Figure 2, a reactor system including a main reactor, a buffer tank, and a side reactor is constructed to simulate COVID-19 transmission in a specific region. The main reactor is considered as semicontinuous if people could move between regions; otherwise, the inlet and outlet flows are assumed to be zero. A time variable $u(t) \in [0, 1]$ is defined as a "diffusion factor" to describe the intensity of molecular diffusion in the reaction system. The system is completely mixed and belongs to reaction control when $u(t) = 1$. $u(t)$ will affect the macroscopic reaction rate of the components linearly in this paper. It is obvious that $u(t)$ also is the intensity of "social distancing" in the epidemic model. It is well-known that the phenomenon of implosion is prone to occur once the concentration of active species in the reactor is too large. Engineers usually design multiple reactors to share the load and ensure the reaction can proceed smoothly. This is like the quarantining of infected patients to avoid large-scale outbreaks of COVID-19. Therefore, we design the side reactor to share the reaction load of some active species in the main reactor. All active species H_m^* and C_m^* are thought to enter the side reactor, and partial reactants I_m^* and E^*, distinguished by subscript q, enter the side reactor with the same ratio $\rho(t) = \frac{\sum E_q^*}{\sum E_q^* + E^*} = \frac{\sum I_q^0}{\sum I_q^0 + I^0}$. $\rho(t)$ represents the intensity of CTI in the epidemic model. Note that there is no monomer $S1$ in the side reactor to generate new active chains, but there are enough monomers $S2$ and polymerization inhibitors A and B for chain propagation and chain deactivation reactions. As a result, an extended model, named SEIR^{+HCQD}, is proposed in Figure 2.

In the above reaction system, N is proposed to represent the total number of molecules except for $S2$, and the formula is shown as eq 21. N is a constant and equal to $S1$ before the reaction occurs

$$N = S1 + E^* + I^0 + H^0 + C^0 + R^0 + D^0 \tag{21}$$

The concentration of reactants is the ratio of number of people to the area of a specific region in our reaction kinetic model. According to Figure 2 and eqs 11−20, the production rate or consumption rate of each component is obtained by eqs 22−30. These equations can describe the transformation relationship between different compartments of people when the area of a specific region is known. In detail, $\frac{d[S1]}{dt}$ represents the derivative of monomer concentration to time, whose unit is $\frac{\text{person}}{\text{d}\cdot\text{km}^2}$. Its value decides on the reaction rate $r_{2,\theta}$, $r_{2m,I}$ and the intensity of "social distancing" $u(t)$. Ignoring the initiator concentration ($k_{i,\theta^*}[\theta^*] \approx 0$) and combining with the above assumption of equal activity, eq 22 can be obtained. Due to the splitting effect of the side reactor, the reaction rate of the intermediate and the active chain (E^* and I^0) is a function of the split ratio, which are expressed by eqs 23−26. The consumed monomer is first transformed into intermediates and then an active chain is generated by the reaction rate φ. In addition to being consumed as a function of k_t and its own concentration, the active chain of the main and side reactors will also be affected by the splitting effect to increase or decrease the actual consumption. Similarly, we can get the consumption or production rate described by eqs 27−30 of the remaining component concentration. Note that considering the difference between the polymerization process and the epidemic spreading process, we assume that the concentration of the polymerization inhibitor meets [A] = 1 and [B] = 1.

$$\frac{d[S1]}{dt} = -u(t)[r_{2,\theta} + \sum r_{2m,I}] = -u(t)k_{i,I_m^*}[S1][I^0] \tag{22}$$

$$\frac{d[E^*]}{dt} = [1 - \rho(t)]\frac{d[S1]}{dt} - r_E = [1-\rho(t)]u(t)k_{i,I_m^*}[S1][I^0] - \varphi[E^*] \tag{23}$$

$$\frac{d[E_q^*]}{dt} = \rho(t)\frac{d[S1]}{dt} - r_E = \rho(t)u(t)k_{i,I_m^*}[S1][I^0] - \varphi[E_q^*] \tag{24}$$

$$\frac{d[I^0]}{dt} = r_E - [1 + \rho(t)]\sum (r_{4m} + r_{5m} + r_{6m}) = \varphi[E^*] - k_t[I^0] - \rho(t)k_t[I^0] \tag{25}$$

$$\frac{d[I_q^0]}{dt} = r_E - [1-\rho(t)]\sum (r_{4m} + r_{5m} + r_{6m}) = \varphi[E_q^*] - k_t[I_q^0] + \rho(t)k_t[I^0] \tag{26}$$

$$\frac{d[H^0]}{dt} = \sum (r_{4m} - r_{7m} - r_{9m} + r'_{9m}) = \alpha\beta k_t([I^0] + [I_q^0]) + (1 - d)k_d[C^0] - k_r[H^0] \tag{27}$$

$$\frac{d[C^0]}{dt} = \sum (r_{5m} - r_{8m} + r_{9m} - r'_{9m}) = \alpha(1 - \beta)k_t([I^0] + [I_q^0]) + \gamma k_r[H^0] - k_d[C^0] \tag{28}$$

$$\frac{d[R^0]}{dt} = \sum (r_{6m} + r_{7m}) = (1 - \alpha)k_t([I^0] + [I_q^0]) + (1 - \gamma)k_r[H^0] \tag{29}$$

$$\frac{d[D^0]}{dt} = \sum r_{8m} = \text{d}\, k_d[C^0] \tag{30}$$

3. PARAMETER ESTIMATION

Estimation of model parameters is a key step in model prediction and optimization. The statistical data of COVID-19 is obtained from the Johns Hopkins University and the official

https://doi.org/10.1021/acs.iecr.1c03647
Ind. Eng. Chem. Res. 2021, 60, 17650−17662

website of the local health department.[22,23] Control variables $u(t)$ and $\rho(t)$ are considered in the regression model due to new NPIs being introduced on a day-to-day basis.[24] Meanwhile, the recovery ratio of hospitalized patients (H) in different periods represented by $1 - \gamma(t)$ is time-varying due to the development of medical treatment. The proportion of deaths of critical patients (C) represented by $d(t)$ will change with the load of ICUs in the medical system. However, infected people (I) will have a fixed proportion of recovery (R) or deterioration (C), which is related to the personal physical quality, which means that α and β are time-independent variables. The objective function is minimizing sum-of-squares of errors between real infection statistics and model calculations. The parameter regression method is described as Model I.

Model I:

$$\text{obj}_{\text{reg}} = \min \sum_{i=1}^{\text{day}} [(R_{\text{real},i} - R_{\text{cal},i})^2 + (D_{\text{real},i} - D_{\text{cal},i})^2 + (\text{Conf}_{\text{real},i} - \text{Conf}_{\text{cal},i})^2] \quad (31)$$

$$\text{s. t.} \quad \text{Conf} = N - S1 \quad (32)$$

Analogy models (eqs 22−30) with $d \rightarrow d(t)$ and $\gamma \rightarrow \gamma(t)$ where Conf represents the cumulative confirmed cases.

To illustrate the procedure of parameter estimation, we employ the early COVID-19 transmission data of three countries or cities including Germany, Maharashtra, and Delhi. The ordinary differential equations (ODEs) of eqs 22−30 are solved using the finite-element orthogonal collocation (OCFE) method with one finite per day to discretize the time domain. The resulting nonlinear programming (NLP) model is implemented in the General Algebraic Modeling System (GAMS) and solved by the generalized reduced gradient algorithm of solver CONOPT4.[25,26] Figure 3 compares the predicted and real values of three selected regions. It is assumed that there is a response period during the initial outbreak of the epidemic in which $u(t) = 1.0$ and $\rho(t) = 0$. It is questionable to calibrate an epidemic model to a single country without migration, but this seems to be justified in a scenario with extensive border closures.[12] According to Figure 3, the value of $\gamma(t)$ approaches 1.0 in the early stage of epidemic that is caused by the lack of knowledge about COVID-19. With the development of specific COVID-19 treatment methods, the possibility of cure for the hospitalized population is gradually increasing and the value of $\gamma(t)$ decreased until stable. In addition, there is an infection period before people recover or die, which leads to a situation where the dead proportion of critical persons $d(t)$ in the initial stage is always equal to zero. After that, there is a sudden increase of $d(t)$ and then a decrease to a lower value. Comparing the fitting results of the three regions, we take $\gamma(t) = 0.2$ and $d(t) = 0.15$ in the following section as long as the capacity of the medical system is enough. Social distancing and contact tracing isolation are two of the NPIs considered in this paper. Both of them will change artificially according to the current situation of COVID-19 transmission. Since the possibility of tracing close contacts varies in $[0, 0.4]$ from day to day, the frequency of changing $\rho(t)$ is relatively higher. In contrast, social distancing is a policy adjustment to the economic activities of the entire region, which generally changes periodically. Combining the statistical test and relative error analysis in Table S1 of the Supporting Information and fitting results of

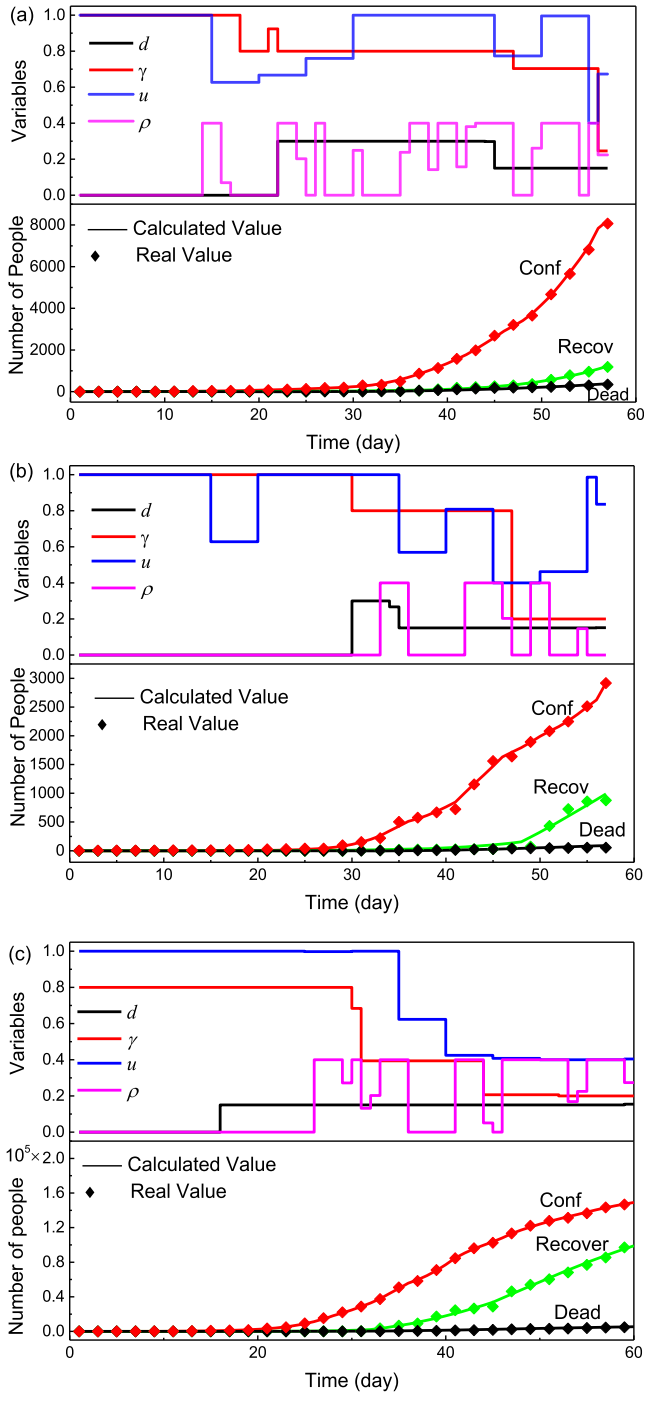

Figure 3. Comparison of model calculated values and real values: Maharashtra, (b) Delhi, and (c) Germany.

Figure 3, the analogy polymerization model can reasonably predict the evolution of the epidemic when parameters such as $d(t)$ and $\gamma(t)$ are considered as time variables. The parameters obtained by the regression model are shown in Table 3.

4. OPTIMIZATION OF CONTROL MEASURES

There are two fundamental issues considered in this section to drive the optimization of control measures. The first one is the capacity of the medical system to deal with the large inflow of patients because COVID-19 does not seem to be an extremely deadly disease once the infected people are treated properly.[27] There are two main methods for handling the medical system

https://doi.org/10.1021/acs.iecr.1c03647
Ind. Eng. Chem. Res. 2021, 60, 17650−17662

Table 3. Model Parameters of Three Regions

symbol	unit	Maharashtra	Delhi	Germany
φ	d^{-1}	0.100	0.142	0.142
$k_{i,Im}^{*}$	$\frac{km^2}{d\cdot person}$	0.020	3.77×10^{-4}	0.027
k_t	d^{-1}	2.0	2.0	2.0
k_r	d^{-1}	0.128	0.180	0.310
k_d	d^{-1}	2.0	0.169	0.127
α		0.87	1.0	1.0
β		0.90	1.0	1.0
N	person	1.22×10^8	2.93×10^7	8.29×10^7
area	km^2	307 700	1484	357 582

capacity in different epidemic situations. One method takes severe measures such as stopping all economic activities in which $u(t) \approx 0$ in the most affected areas to minimize the number of infected people, another one implemented the flexible policies to slow the spread of infection aiming to avoid the overload of the medical system and paralysis of the city's economy. The second one is the tradeoff between economic costs and the number of deaths due to COVID-19. Although strict social distancing can effectively curb the transmission of epidemics, it also reduces economic outputs due to the corresponding reduction in economic activities. Testing the entire population simultaneously to find all virus carriers and quarantining them would eliminate the second problem directly, but it is difficult and extremely expensive in current conditions. Therefore, what measures should be taken to prevent the capacity overload of the medical system? How strict and how long should those measures be? All of these should be optimized.

4.1. Temporal Evolution Curves of Different NPIs. According to eq 30 of Section 2 for the analogy of the spreading process of COVID-19 with the polymerization system, it can be known that the number of deaths (D) depends on the number of critical patients (C) and the mortality ratio $d(t)$. $d(t)$ is determined by the number of ICUs and critical patients. Let d_1 represent the mortality ratio of critical patients with ICUs and d_2 is the one without ICUs. As a result, the average mortality ratio can be calculated by eq 33

$$d(t) = d_1 \min\left\{1, \frac{C_0}{C(t)}\right\} + d_2 \max\left\{1 - \frac{C_0}{C(t)}, 0\right\} \quad (33)$$

where C_0 is the total number of ICUs in the regions or countries affected by COVID-19. According to the results of parameter regression, $d_1 = 0.15$, and according to xx et al.,[3] $d_2 = 2d_1$.

Before we optimize the operating conditions of reactors, it is necessary to study the profiles of various operating points. Similarly, we first study the time-varying curves of the compartment population under different NPIs and take Maharashtra as an example. The model parameters used are from Table 3. According to the statistics of ICUs given by the Society of Critical Care Medicine (SCCM),[28] the number of ICUs per 100 000 inhabitants ξ_{ICU} is 2.3 in Maharashtra. Figure 4 gives the simulation results about the evolution of each compartment population in 500 days when different NPIs are implemented. The shadowed areas represent the simulated results in kinetic parameter regression section, which are used to give the initial value of each population. Based on the different levels of SD and CTI, there are five scenarios from Figure 4a to e for controlling epidemics. Note that both the exposed and infected populations in Figure 4 include those in isolation. Comparing the peak values of curves, appropriate measures such as those in Figure 4b,c,e can make the epidemic controllable immediately, and the number of infected people will also show a downward trend. Otherwise, the epidemic will continue to spread for a while, and the number of infections will reach a higher peak like in Figure 4a,d. On the other hand, we keep one of the two measures (SD and CTI) at a constant level and further study the influence of the intensity of another measure. Comparing Figure 4a–c, when SD is in a state of nonintervention for $u(t) = 1.0$, the peak of infected people will be as high as 5.86×10^5, and the final deaths will account for 5.7% of the total population. However, the peak of infected people will be reduced to around 200 once the government reduces SD by a half, which will cause less than 2000 deaths due to COVID-19. When further reducing SD to $u(t) = 0.1$, although the peak of infections will not be reduced more, the duration of the epidemic will be greatly reduced. From the perspective of polymerization, this is similar to the scenario where the reaction of active species and monomers is affected

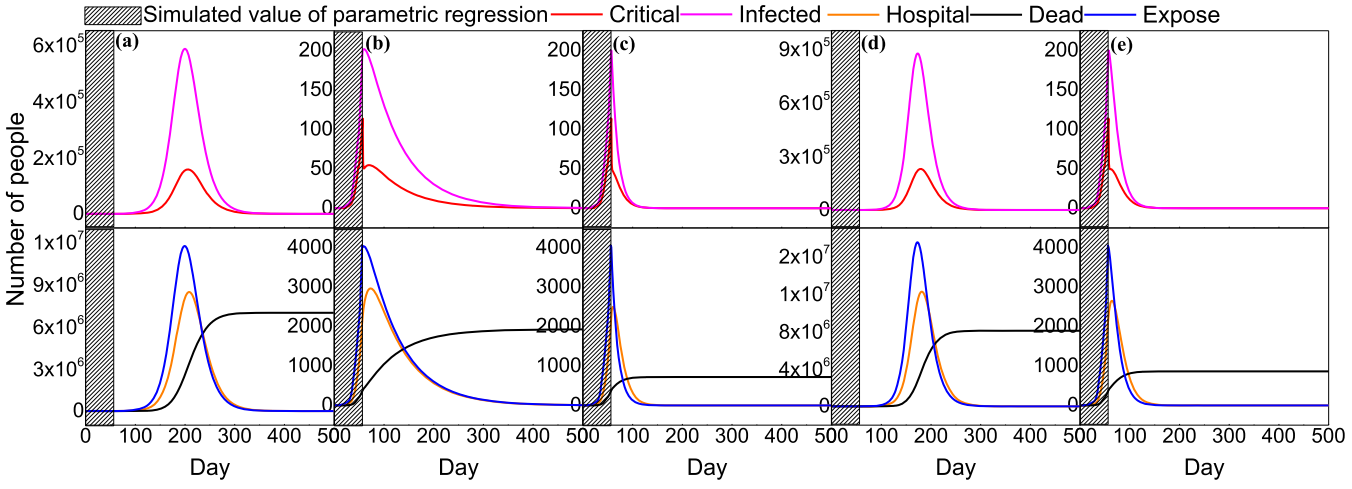

Figure 4. Effects of SD and CTI in Maharashtra with (a) $u = 1.0$ and $\rho = 0.4$, (b) $u = 0.5$ and $\rho = 0.4$, (c) $u = 0.1$ and $\rho = 0.4$, (d) $u = 0.5$ and $\rho = 0$, and (e) $u = 0.5$ and $\rho = 0.8$.

https://doi.org/10.1021/acs.iecr.1c03647
Ind. Eng. Chem. Res. 2021, 60, 17650−17662

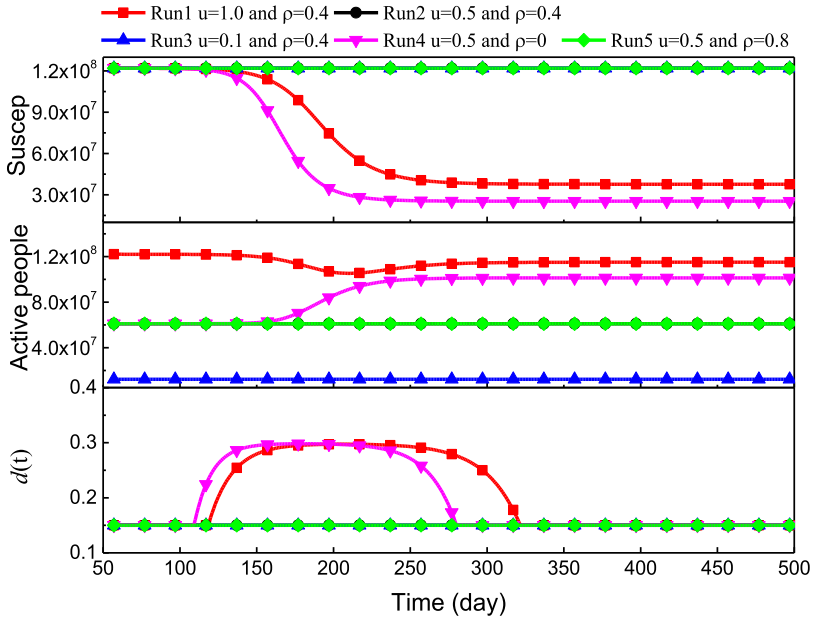

Figure 5. Evolution curves of different measures in Maharashtra.

Table 4. Population Growth with Different Response Times

	Maharashtra			Delhi			Germany		
	dead	recover	conf	dead	recover	conf	dead	recover	conf
$t = 0$	385	1225	8207	89	988	2917	4830	87 745	143 019
$R_t = 10$	3231	63 073	66 452	1776	33 628	35 419	20 733	468 513	489 362
$R_t = 20$	36 821	733 517	774 251	51 700	709 433	761 935	282 871	4 213 813	4 499 810
$R_t = 30$	688 058	8 109 414	8 886 560	754 308	10 103 623	10 878 438	2 221 188	30 264 924	32 527 673

by the diffusion rate. The greater the barrier to diffusion, the less the polymer formed. In addition, based on the adjustment of the concentration of active species in the reactor to prevent reactor explosion, isolating infected persons is like transferring active chains I_m to a side reactor, which has a lack of monomers $S1$. Research on the influence of the intensity of CTI is shown in Figure 4b,d,e. When SD is at a moderate level such as $u(t) = 0.5$, the peak of infected people would exceed 8.73×10^5 if no tracking and isolation measures are taken such as $\rho(t) = 0$. In addition, the higher the intensity of CTI, the lower the peak of infections and the shorter the duration of the epidemic. Therefore, we can conclude that under the premise of a certain intensity, both measures are effective in restraining the spread of epidemics.

The above discussion proves that taking effective control measures can cut off the virus transmission theoretically. However, the economic costs associated with these control measures cannot be ignored. We measure the economic costs by the number of active people. Let $\Omega(t)$ denote the people who can carry out normal economic activities under control measures at time t. Also, let TEO^{t_f} represent the total economic output of a specific region during the period $[0, t_f]$ under the control measures. $\Omega(t)$ and TEO^{t_f} can be calculated as

$$\Omega(t) = u(t)[S1(t) + E(t) + I(t)] + R(t) \tag{34}$$

$$\mathrm{TEO}^{t_f} = \int_0^{t_f} \eta\Omega(t)\,\mathrm{d}t \tag{35}$$

where coefficient η is used to represent GDP for one person per day.

Figure 5 shows the evolution curves of active people, susceptible population, and $d(t)$ under different SDs and CTIs described as Run1−Run5. There are no obvious fluctuations on active people, susceptible population, and $d(t)$ in Run2, Run3, and Run5 in which the control measures are in a higher level. From the perspective of polymerization, it represents the reaction steps quickly but there is still a large amount of unreacted monomer $S1$ in the reactor, which will cause secondary reactions once the initiator is introduced again. This is called unrealized herd immunity in epidemiology. On the contrary, if minor control measures such as Run1 and Run4 are taken, the mortality ratio $d(t)$ would increase in a period due to insufficient capacity of the medical system. Meanwhile, the herd immunity could be achieved eventually in which most susceptible people are transformed into recovered people. Further comparing the curve trends of run1 and run4, CTI seems to be more advantageous than SD when only one measure is taken. The cumulative number of infections caused by CTI is less than that of SD, and the number of people in the active state is also more. Figures S1−S4 of the supporting information give more detailed information of simulation results including Germany, Delhi, and Maharashtra.

4.2. Response Time Measurement. It is an effective method to block the infected area and maintain strict measures when there is a sudden epidemic. Currently, the response time becomes the main factor affecting the effectiveness of epidemic prevention and control. In this section, we assume that no interventions are implemented during the response period, which means $u(t) = 1.0$ and $\rho(t) = 0$. After that, 90% of people are in self-isolation except for inevitable activities, which means

https://doi.org/10.1021/acs.iecr.1c03647
Ind. Eng. Chem. Res. 2021, 60, 17650−17662

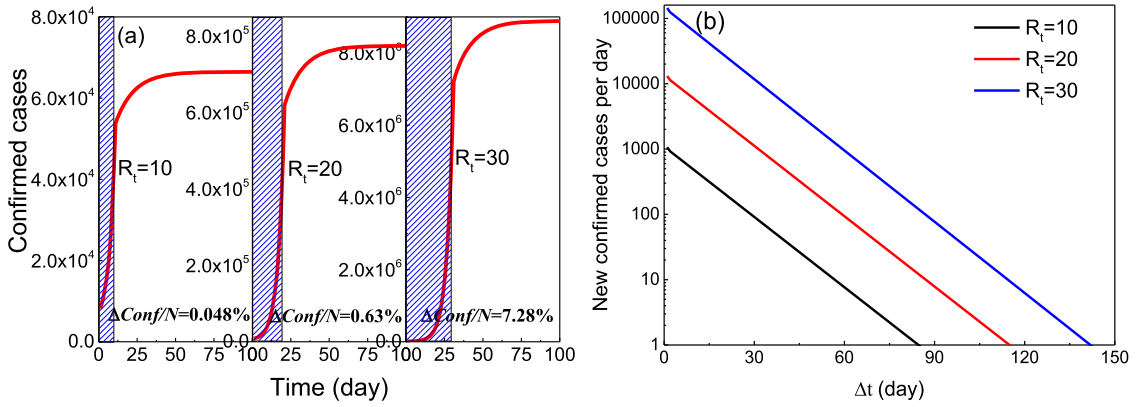

Figure 6. Confirmed cases (a) and newly confirmed cases per day (b) with various response times in Maharashtra.

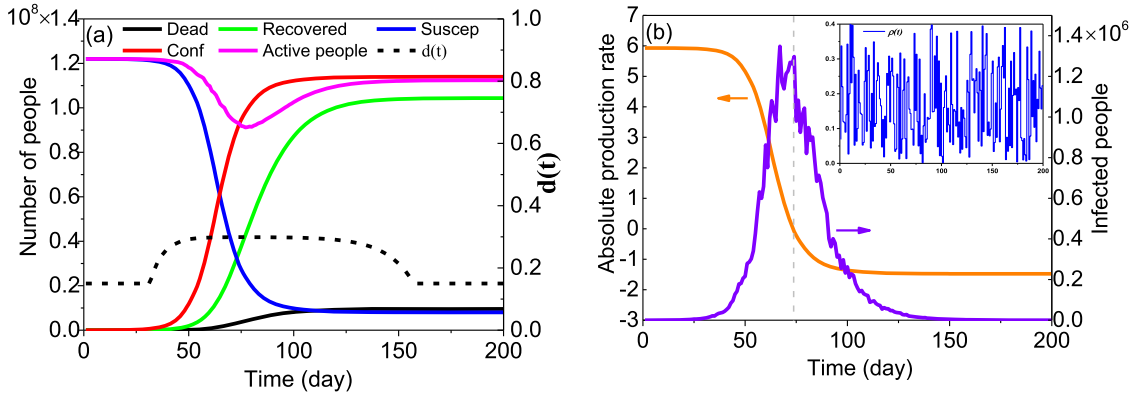

Figure 7. Simulated natural evolution in Maharashtra: (a) compartment population and $d(t)$ and (b) absolute production rate and infected people.

$u(t)$ = 0.1. Meanwhile, the value of $\rho(t)$ is related to the efficiency of infection tracking and testing and the real-time proportion of infected persons. $\rho(t)$ is random but this part makes its value 0.4. Based on the above assumptions and the results of parameter estimation in Section 3, the impact of response time in Maharashtra, Germany, and Delhi on the development of epidemics is researched. The simulation results of the 57th day in three regions in Section 3 are selected as the initial value of each population in this study. The response times are 10, 20, and 30 days, respectively. Table 4 shows the simulation results on the 100th day of the dead, recovered, and confirmed population under different response times. When the response time increases from 10 to 20 days, confirmed people of three regions will increase by 11, 21, and 9 times, respectively. If the response time further increases from 20 to 30 days, confirmed people in Maharashtra will maintain the same growth ratio, while Delhi and Germany's growth ratio will reduce to 14 and 7 times. This is due to different initial infection conditions. When corresponding measures are taken, the growth ratio of confirmed cases will gradually reduce to zero. This is similar to the S-shaped growth curve for the polymer in the autocatalytic polymerization system. The polymer will grow exponentially due to burst with enough monomers until the monomers and active species become insufficient. Figure 6a shows the evolution curves in Maharashtra and the S-shaped growth curve can be observed. We define ΔConf to represent the difference in the number of confirmed cases among 100 days. The shaded parts indicate the response time interval. According to Figure 6a, the number of confirmed cases increases exponentially during the response time. Once strict control measures are taken, the growth rate will immediately slow down. For each 10-day increase in response time, the number of confirmed people within 100 days will increase by 10 times. Figure 6b shows the relationship between the number of new confirmed cases per day and the response time. The abscissa represents the cumulative days of implementing strict control measures. The epidemic can be considered to end once the number of new confirmed cases per day is less than 1 for several consecutive days. It takes about 85, 115, and 142 days to eliminate the epidemic when the response times are 10, 20, and 30 days, respectively. This means that the sooner the measures are taken, the sooner the epidemic will end.

4.3. Establish Herd Immunity. *4.3.1. Natural Evolution.* In this part, we assume that the government does not take any measure except for isolating the exposed and infected people through contact tracing. The value of $\rho(t)$ varies from 0 to 0.4 randomly every day due to the volatility itself. Figure 7 describes the results of natural evolution in Maharashtra, which includes the time-varying curves of different compartment population, active people, and absolute generation rate Ψ of infected people. The initial values of this natural evolution research are also from the results of Section 3. The absolute generation rate is related with susceptible persons and calculated by eq 36

$$\Psi = k_{i,I_m^*}[S1] - k_t \tag{36}$$

According to eqs 23−26, when the value of Ψ is less than zero, it means that the number of infected persons will gradually decrease to zero even if the control measures meet $u(t) \equiv 1.0$

https://doi.org/10.1021/acs.iecr.1c03647
Ind. Eng. Chem. Res. 2021, 60, 17650−17662

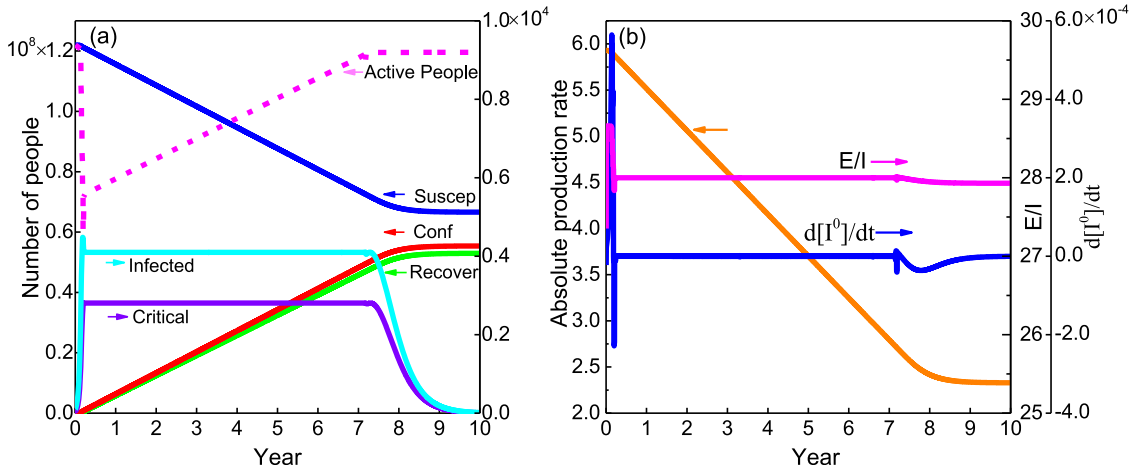

Figure 8. Long-term control optimization results in Maharashtra: (a) compartment population and (b) absolute production rate.

and $\rho(t) \equiv 0$. This status is called herd immunity in epidemiology. In Figure 7a, the number of active people is always at a higher level, and the smallest proportion to the total population is 74.7%. This is caused by everyone's normal participation in economic activities except for critical and hospitalized people. The number of confirmed cases increases exponentially and approaches the limit quickly, which means herd immunity. Figure 7b shows that the time required for herd immunity is 74 days. Although the economic loss of natural evolution is small and herd immunity can also be obtained as soon as possible, the explosive increase in confirmed cases has overloaded the local medical system, and most patients hardly receive effective treatment. The mortality ratio $d(t)$ will remain at a high level for a long time and the final number of deaths is as high as 9.57×10^6, accounting for 8.4% of the total number of infections. This is unacceptable for the government in actual situations.

4.3.2. Control Interventions. It is impractical to take no intervention to deal with the epidemic. Before the vaccine is successfully developed and put into use, NPIs are the main method for the government to control the spread of epidemics. Meanwhile, there is a tradeoff between the economic costs and the corresponding measures. In this part, Model II is proposed to coordinate the positive effects of social distancing on the spread of epidemics and the negative effects on economic output.

Model II:

$$\mathrm{obj}_{\mathrm{int}} = \max_{u,\rho} \mathrm{TEO}^{t_f} | \eta = 1 \tag{37}$$

$$\text{s. t. } D \le D_{\max} \text{ or } \frac{D}{\mathrm{Conf}} \le \left(\frac{D}{\mathrm{Conf}}\right)_{\max} \tag{38}$$

$$C \le C_{\max} = \frac{\xi_{\mathrm{ICU}} N}{100\,000} \tag{39}$$

Analogy models (eqs 22−30) with $d \to d(t)$ by eq 33

where $u(t)$ is the decision variable and changes every 5 days in [0.1, 1.0] and $\rho(t)$ is random and changes everyday in [0, 0.4]. $D_{\max}$ is the upper bound of the acceptable number of deaths and $C_{\max}$ is the upper bound of the number of critical patients, which is decided by the total population of the region and the proportion of the ICUs.

To consider the possibility of realizing herd immunity without vaccines, the time interval of Model II is designed to 10 years. Figure 8 shows the results of optimizing SD trajectories to maximize TEO^{t_f} in Maharashtra when the constraints meet $\left(\frac{D}{\mathrm{Conf}}\right)_{\max} = 0.05$ and $\xi_{\mathrm{ICU}} = 2.3$. Figure 8a shows the evolution curve of each compartment and Figure 8b gives the absolute production rate, the ratio of exposed population to infected population, and the value of $\frac{\mathrm{d}[I^0]}{\mathrm{d}t}$. According to Figure 8a, the number of susceptible people is declining, while the number of recovered and confirmed people are increasing. The number of infected and critical patients remains unchanged for a long time and eventually decrease to zero. Obviously, the medical system can always operate normally due to the corresponding constraint for critical patients. This means that susceptible people are transformed into immune recovered people within a steady rate. Once the epidemic is in a controllable range, the constraints of SD will be gradually released to obtain higher economic output, which is reflected in the gradual increase in the number of active people. However, the value of Ψ is greater than zero all the time from Figure 8b, which means that the society ultimately has not achieved herd immunity, according to the conclusion in natural evolution research. The reason that makes the number of infected people be eventually cleared is that the generation rate of the number of infected people $\left(\frac{\mathrm{d}[I^0]}{\mathrm{d}t}\right)$ will be less than zero after 7.5 years, and the necessary condition is the value of E/I that is less than 27.9. When the virus reappears, we cannot guarantee that its spread will be naturally blocked due to the uncertainty of the new value of E/I. Therefore, this situation is defined as quasi-herd immunity in which the epidemic still has the possibility of a small secondary outbreak.

4.3.3. Measure Optimization with Vaccination. After the vaccines are put into use, the impact of vaccination is considered in Model II. Continuous and impulsive vaccination have been proposed among previous papers.[29−31] The strategy of continuous vaccination, in which the susceptible population is vaccinated at a continuous immunization rate δ, is not realistic since the population is vaccinated only at discrete time points.[32] Therefore, a form of impulsive vaccination is considered and the new optimization Model III is established as following. Inequality constraints (eqs 38 and 39) are considered at the same time.

Model III:

https://doi.org/10.1021/acs.iecr.1c03647
Ind. Eng. Chem. Res. 2021, 60, 17650−17662

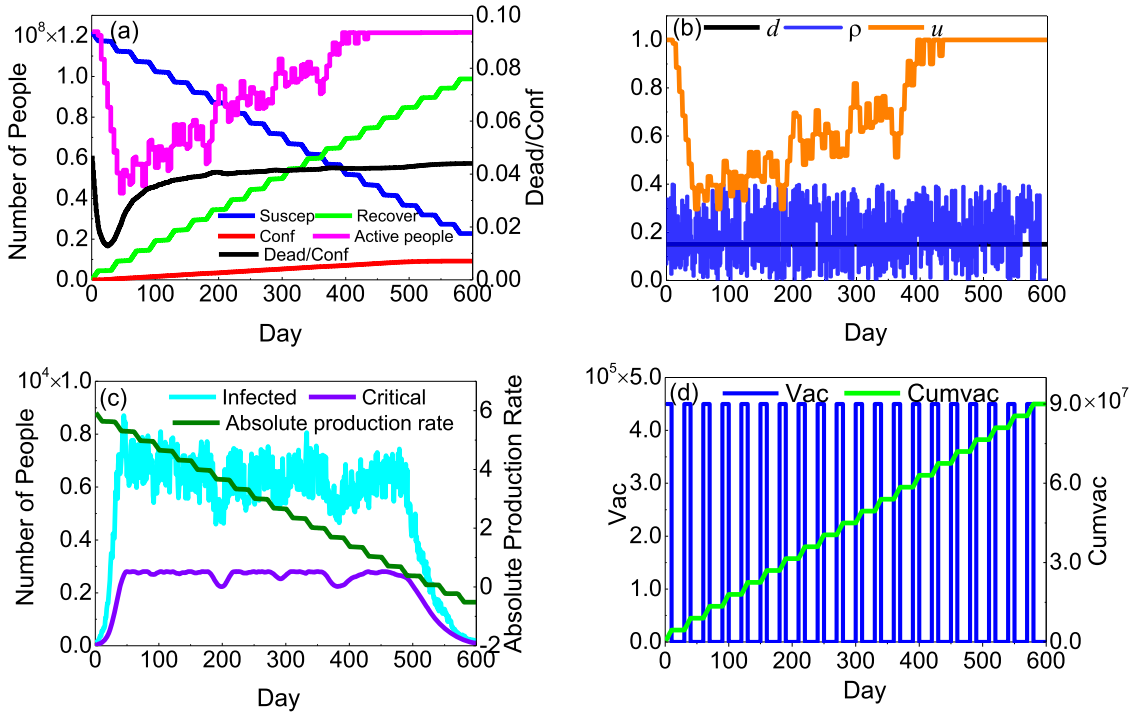

Figure 9. Optimization results of Model III with vaccination in Maharashtra $\left(\frac{D}{\text{Conf}}\right)_{\max} = 0.05$, $P_{\max} = 10$, and $\text{vac}_{\max} = 4.5 \times 10^5$: (a) compartment population and death ratio, (b) control measures, (c) infected and critical people and absolute production rate, and (d) vaccination strategy.

Table 5. Initial Conditions of the Three Regions

item	suscep	expose	Qexpose	infected	Qinfected	hospital	critical	recover	dead	area/m^2
region 1	24 398 360	586	217	21	19	454	23	245	77	61 540
region 2	36 597 540	879	325	32	28	681	34	368	116	92 310
region 3	60 995 900	1464	542	54	46	1135	57	613	193	153 850

$$\text{obj}_{\text{vac}} = \max_{u,\rho} \text{TEO}^{t_f} | \eta = 1 \tag{40}$$

$$\text{s. t. } S1_{l+1} = S1_l - \text{vac}_l \tag{41}$$

$$R_{l+1}^0 = R_l^0 + \text{vac}_l \tag{42}$$

$$\text{vac}_l - B_l \text{vac}_{\max} \le 0 \tag{43}$$

$$\sum_{l=1+30k}^{30+30k} B_l - P_{\max} \le 0, \quad k = 0, 1, 2, ..., K \tag{44}$$

Analogy models (eqs 22−30) with $d \to d(t)$ by eq 33

where vac_l indicates the number of people vaccinated on the lth day. B_l is a binary variable for deciding whether there is a centralized vaccination on the lth day. $\text{vac}_{\max}$ represents the maximum number of vaccines per day and $P_{\max}$ represents the maximum feasible vaccinated days during each vaccination cycle (30 days). k represents the $k + 1$ vaccination cycle. The time interval of Model III is also large enough such as $K \ge 15$ to complete the establishment of herd immunity.

In this section, we couple 0−1 variables with ODEs to simulate the actual situation more realistically and call the solver DICOPT to solve the corresponding mixed integer nonlinear programming (MINLP).[33] The result is shown in Figure 9 with the related constraints given. Figure 9a shows the time-varying curves of each compartment population in 600 days. Both susceptible and recovered population change in the form of pulses due to the pulsed vaccination. In addition, there are fewer people with immunity in the early stage, so the government should restrict social distancing to avoid a surge in the number of infected people. Therefore, the number of active people is small until the epidemic is in a controllable stage, when social distancing restrictions are reduced to obtain more economic outputs. Figure 9b shows the trajectories of two control measures and the mortality ratio. Because the corresponding intervention measures ensure the normal operation of the medical system, $d(t)$ is always at the lowest level. The trajectory of $u(t)$ is similar to the number of active people due to the linear relationship between them. Figure 9c shows the trend of another two-compartment population and absolute production rate Ψ. The number of infected people can be observed to fluctuate significantly, which is caused by contact tracing isolation and the value of $\rho(t)$ is random. Meanwhile, it takes 500 days to keep Ψ less than zero and achieve herd immunity. Compared with natural evolution, the final number of deaths can be reduced to original 4.24%. The value of the objective function to total population $\left(\frac{\text{TEO}^{t_f}}{N}\right)$ is 473.61, which means that the average daily economic output is reduced by 21.1% compared to the normal situation. The optimization result of impulsive vaccination is shown in Figure 9d. It is obvious that vaccinations always occur in the first 10 days of each month and the number of vaccines used per day is equal to the upper bound. According to Figure 9d, the upper bound of vaccines and maximum days of vaccination per

https://doi.org/10.1021/acs.iecr.1c03647
Ind. Eng. Chem. Res. 2021, 60, 17650−17662

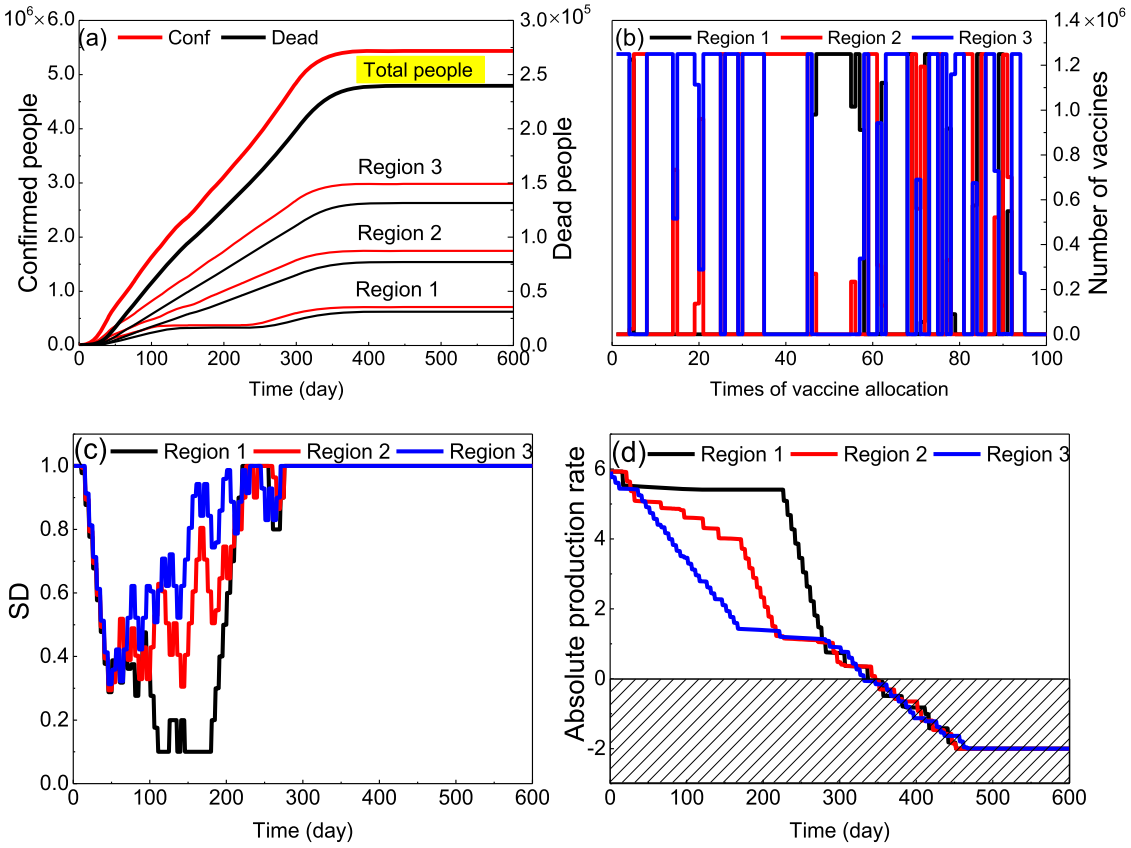

Figure 10. Optimization results of the vaccine allocation model, $\left(\frac{D}{\text{Conf}}\right)_{\max} = 0.05$ and $\text{vac}'_{\max} = 1.25 \times 10^6$: (a) confirmed and dead people in different regions, (b) vaccination allocation strategy, (c) social distancing trajectories, and (d) absolute production rate.

month are the main factors that affect the control result. Figure S7 gives the detailed simulation results in the Supporting Information.

Due to the differences in the form and intensity of epidemic control measures in different regions, the epidemic situation among different regions is also different. Therefore, it is necessary to carry out reasonable scheduling of vaccines. Maharashtra is divided into three regions whose initial values are different and are shown in Table 5 to research the multiregion optimization. We assume that the total number of vaccines given to the three regions in 5 days is a constant, and the distribution measures are also updated every 5 days. Replacing constraint eqs 43 and 44 by eq 45, Model III becomes the vaccine allocation model

$$\sum_{j} \sum_{l=1+5k}^{l=5+5k} \text{vac}_{j,l} - \text{vac}'_{\max} \le 0,\ k = 0, 1, 2, \ldots, K \tag{45}$$

where j represents the jth region, and $\text{vac}'_{\max}$ is the upper bound of the total number of vaccines for all of the regions.

According to Table 5, the compartment populations in Regions 1, 2, and 3 account for 20, 30, and 50% of the corresponding ones in Maharashtra. Figure 10a,b shows the time-varying curves of confirmed and dead cases and vaccine allocation curves in the three regions, respectively. The vaccine will be allocated more to the region with more infected and exposed people (Regions 2 and 3) at the initial stage. For Region 1, it is more reasonable to implement strict social distancing to control the spread of the epidemic because the economic loss caused by the same intensity NPIs is smaller than in the other two regions. Therefore, it can be observed that the intensities of SD in Regions 2 and 3 are higher than in Region 1 in Figure 10c. Based on Figure 10a,d, all of the regions will reach herd immunity around the 348th day and the number of confirmed cases will be stable after that day. The value of the objective function to total population $\left(\frac{\text{TEO}^{tf}}{N}\right)$ is 525.98. The result of the corresponding case for comparison in which the vaccine distribution is not considered is shown in Figure S8 in the Supporting Information. The value of $\frac{\text{TEO}^{tf}}{N}$ in the comparison case is 522.87.

5. CONCLUSIONS

Based on the similarity between the S-shaped growth curve of the confirmed people in an epidemic and the polymer concentration in free-radical polymerization, this paper uses a polymerization reaction to simulate the epidemic successfully by comparing compartment populations as reactants or products. This analogy provides a new theoretical perspective for the control optimization of epidemics. We analyze and study three regions of Maharashtra, Delhi, and Germany and obtain the corresponding mechanism model that predicts the characteristics of epidemic transmission (including peak value, duration, etc.). Strategies of pharmacological and non-pharmacological interventions have been optimized and the main conclusions include:

1. With different intensities of nonpharmaceutical interventions, the development of the epidemic will be separated into two trends. At higher intensity

https://doi.org/10.1021/acs.iecr.1c03647
Ind. Eng. Chem. Res. 2021, 60, 17650−17662

interventions ($u \leq 0.5$ or $\rho \geq 0.4$), the number of infected persons will rapidly decrease from peak to zero; under lower intensity interventions ($u > 0.5$ or $\rho < 0.4$), the number of infected individuals will continue to rise for a while until a higher peak is achieved. In addition, similar to radical polymerization, the transmission process of the epidemic has sigmoidal growth curve properties. The response time is a major factor influencing the peak number of confirmed people and duration of the epidemic. The longer the response time, the more likely an epidemic is to undergo exponential growth, the greater its number of confirmed people, and the longer its duration.

2. Without taking any nonpharmaceutical interventions other than contact tracing and isolation, herd immunity can be achieved less than 100 days through natural evolution in the above three regions, but this will cause more than 90% of the people to be infected and the collapse of the medical system. Taking some NPIs and optimizing the intensity of social distancing to maximize the economic output within the acceptable cost, the normal operation of the medical system is ensured and it will take several years to eliminate epidemics; however, it cannot guarantee the realization of herd immunity.
3. Combining pulse vaccination and nonpharmaceutical interventions is the most effective method to achieve herd immunity in a short period without a high proportion of infections. In this way, only 8% of the total population will eventually be infected. The available vaccines per day and the number of pulse vaccination are the main factors that affect the time for herd immunity. A reasonable allocation of vaccines to different regions in which epidemic development trends are different can better coordinate the effects among control measures, further reduce the number of confirmed people and deaths, and increase the overall economic output.

Actually, based on the analogy between epidemics and the free-radical polymerization reaction, there are many research directions in the future. For example, considering the activity difference in different active chains, the difference of the virus transmission rate among patients infected for different days can be explored. Meanwhile, it is also feasible to study the optimization of epidemic control under the conditions of population movement between different regions through the link between the reactors and the exchange of materials.

■ ASSOCIATED CONTENT

Supporting Information

The Supporting Information is available free of charge at https://pubs.acs.org/doi/10.1021/acs.iecr.1c03647.

Model feasibility test, simulation results of Delhi and Germany, and the multiregion optimization comparison case (PDF)

■ AUTHOR INFORMATION

Corresponding Author

Zuwei Liao − *State Key Laboratory of Chemical Engineering, College of Chemical and Biological Engineering, Zhejiang University, Hangzhou 310027, China;* orcid.org/0000-0001-9063-1049; Email: liaozw@zju.edu.cn

Authors

Chijin Zhang − *State Key Laboratory of Chemical Engineering, College of Chemical and Biological Engineering, Zhejiang University, Hangzhou 310027, China*

Jingyuan Sun − *State Key Laboratory of Chemical Engineering, College of Chemical and Biological Engineering, Zhejiang University, Hangzhou 310027, China;* orcid.org/0000-0002-8876-9951

Yao Yang − *State Key Laboratory of Chemical Engineering, College of Chemical and Biological Engineering, Zhejiang University, Hangzhou 310027, China;* orcid.org/0000-0003-3611-2859

Jingdai Wang − *State Key Laboratory of Chemical Engineering, College of Chemical and Biological Engineering, Zhejiang University, Hangzhou 310027, China;* orcid.org/0000-0001-8594-4286

Yongrong Yang − *State Key Laboratory of Chemical Engineering, College of Chemical and Biological Engineering, Zhejiang University, Hangzhou 310027, China;* orcid.org/0000-0002-5598-6925

Complete contact information is available at: https://pubs.acs.org/10.1021/acs.iecr.1c03647

Notes

The authors declare no competing financial interest.

■ ACKNOWLEDGMENTS

The financial supports provided by the Project of the National Natural Science Foundation of China (21822809 and 21978256) and the Ningxia Hui Autonomous Region Key Research and Development Program (2019BFH02016) are gratefully acknowledged.

■ NOMENCLATURE

u	intensity of social distancing at time t
ρ	proportion of people quarantined through contact tracing at time t
S	monomer divided into $S1$ and $S2$
m	length of active chains
I_m^*, H_m^*, C_m^*	active chain molecules
Θ	initiator molecule
ϑ^*	primary free radicals generated by the initiator
ϑ_d	inactivated small molecules
E^*	intermediate of monomer free radicals
A, B	polymerization inhibitor
D_m, R_m	deactivated polymer
r_i	elementary reaction rate
k_{i,ϑ^*}, $k_{i,Im}^*$	chain initiation rate constant
$k_{p,F}$	chain propagation rate constant
k_t	chain transfer rate constant
k_r, k_d	chain inactivation rate constant
n	moment model superscript
[]	component concentration, person/m^2
SD	social distancing
CTI	contact tracing isolation
N	total population of specific region
Conf	cumulative confirmed cases of COVID-19
C_0	number of ICUs in a region
$\Omega(t)$	active population at time t
TEO^{t_f}	total economic output in a period $[0, t_f]$
R_t	response time, day
η	GDP for one person per day

Ψ absolute generation rate of infected people

REFERENCES

(1) Chen, J. Pathogenicity and transmissibility of 2019-nCoV—a quick overview and comparison with other emerging viruses. *Microbes Infect.* **2020**, *22*, 69−71.

(2) Monari, C.; Gentile, V.; Camaioni, C.; Marino, G.; Coppola, N.; Vanvitelli COVID. A focus on the nowadays potential antiviral strategies in early phase of coronavirus disease 2019 (Covid-19): A narrative review. *Life* **2020**, *10*, No. 146.

(3) Piguillem, F.; Shi, L. Optimal COVID-19 quarantine and testing policies. CEPR Discussion Paper No. DP14613, 2020, 1−44. Available at SSRN: https://ssrn.com/abstract=3594243.

(4) Holmdahl, I.; Buckee, C. Wrong but useful—what covid-19 epidemiologic models can and cannot tell us. *N. Engl. J. Med.* **2020**, *383*, 303−305.

(5) Ribeiro, M. H. D. M.; da Silva, R. G.; Mariani, V. C.; dos Santos Coelho, L. Short-term forecasting COVID-19 cumulative confirmed cases: Perspectives for Brazil. *Chaos, Solitons Fractals* **2020**, *135*, No. 109853.

(6) Chakraborty, T.; Ghosh, I. Real-time forecasts and risk assessment of novel coronavirus (COVID-19) cases: A data-driven analysis. *Chaos, Solitons Fractals* **2020**, *135*, No. 109850.

(7) Wu, J. T.; Leung, K.; Leung, G. M. Nowcasting and forecasting the potential domestic and international spread of the 2019-nCoV outbreak originating in Wuhan, China: a modelling study. *Lancet* **2020**, *395*, 689−697.

(8) Sarkar, K.; Khajanchi, S.; Nieto, J. J. Modeling and forecasting the COVID-19 pandemic in India. *Chaos, Solitons Fractals* **2020**, *139*, No. 110049.

(9) Giordano, G.; Blanchini, F.; Bruno, R.; Colaneri, P.; Di Filippo, A.; Di Matteo, A.; Colaneri, M. Modelling the COVID-19 epidemic and implementation of population-wide interventions in Italy. *Nat. Med.* **2020**, *26*, 855−860.

(10) Liu, Z.; Magal, P.; Seydi, O.; Webb, G. A COVID-19 epidemic model with latency period. *Infect. Dis. Modell.* **2020**, *5*, 323−337.

(11) Peng, L.; Yang, W.; Zhang, D.; Zhuge, C.; Hong, L. Epidemic analysis of COVID-19 in China by dynamical modeling. 2020, arXiv:2002.06563. arXiv.org e-Print archive. https://arxiv.org/abs/2002.06563 (accessed Feb 16, 2020).

(12) Gill, B. S.; Jayaraj, V. J.; Singh, S.; Mohd Ghazali, S.; Cheong, Y. L.; Md Iderus, N. H.; Labadin, J. Modelling the effectiveness of epidemic control measures in preventing the transmission of COVID-19 in Malaysia. *Int. J. Environ. Res. Public Health* **2020**, *17*, No. 5509.

(13) Shim, E.; Tariq, A.; Choi, W.; Lee, Y.; Chowell, G. Transmission potential and severity of COVID-19 in South Korea. *Int. J. Infect. Dis.* **2020**, *93*, 339−344.

(14) Kantner, M.; Koprucki, T. Beyond just "flattening the curve": Optimal control of epidemics with purely non-pharmaceutical interventions. *J. Math. Ind.* **2020**, *10*, No. 23.

(15) Gani, R.; Bałdyga, J.; Biscans, B.; Brunazzi, E.; Charpentier, J. C.; Drioli, E.; Woodley, J. M.; et al. A multi-layered view of chemical and biochemical engineering. *Chem. Eng. Res. Des.* **2020**, *155*, A133−A145.

(16) Manenti, F.; Galeazzi, A.; Bisotti, F.; Prifti, K.; Dell'Angelo, A.; Di Pretoro, A.; Ariatti, C. Analogies between SARS-CoV-2 infection dynamics and batch chemical reactor behavior. *Chem. Eng. Sci.* **2020**, *227*, No. 115918.

(17) Willis, M. J.; Wright, A.; Bramfitt, V.; Díaz, V. H. G. COVID-19: Mechanistic model calibration subject to active and varying non-pharmaceutical interventions. *Chem. Eng. Sci.* **2021**, *231*, No. 116330.

(18) Pandey, G.; Chaudhary, P.; Gupta, R.; Pal, S. SEIR and Regression Model based COVID-19 outbreak predictions in India. 2020, arXiv:2004.00958. arXiv.org e-Print archive; https://arxiv.org/abs/2004.00958 (accessed April 1, 2020).

(19) Bodke, A. S.; Olschki, D. A.; Schmidt, L. D.; Ranzi, E. High selectivities to ethylene by partial oxidation of ethane. *Science* **1999**, *285*, 712−715.

(20) Bamford, C. H.; Tompa, H. On the calculation of molecular weight distributions from kinetic schemes. *J. Polym. Sci.* **1953**, *10*, 345−350.

(21) Bamford, C. H.; Tompa, H. The calculation of molecular weight distributions from kinetic schemes. *Trans. Faraday Soc.* **1954**, *50*, 1097−1115.

(22) Government of Maharashtra Public Health Department. 2020. https://arogya.maharashtra.gov.in (retrieved April 27, 2020).

(23) Government of National Capital Territory of Delhi. 2020. https://delhi.gov.in (retrieved April 27, 2020).

(24) Kermack, W. O.; McKendrick, A. G. Contributions to the mathematical theory of epidemics. II.—The problem of endemicity. *Proc. R. Soc. London, Ser. A* **1932**, *138*, 55−83.

(25) Britz, W.; van der Mensbrugghe, D. CGEBox: A flexible, modular and extendable framework for CGE analysis in GAMS. *J. Global Econ. Anal.* **2018**, *3*, 106−177.

(26) Drud, A. CONOPT: A GRG code for large sparse dynamic nonlinear optimization problems. *Math. Program.* **1985**, *31*, 153−191.

(27) Cortegiani, A.; Ingoglia, G.; Ippolito, M.; Giarratano, A.; Einav, S. A systematic review on the efficacy and safety of chloroquine for the treatment of COVID-19. *J. Crit. Care* **2020**, *57*, 279−283.

(28) Society of Critical Care Medicine. United States Resource Availability for COVID-19. https://www.sccm.org/Communications/Critical-Care-Statistics (accessed Aug 30, 2020).

(29) Yusuf, T. T.; Benyah, F. Optimal control of vaccination and treatment for an SIR epidemiological model. *World J. Modell. Simul.* **2012**, *8*, 194−204.

(30) Liu, H.; Yu, J.; Zhu, G. Global stability of an age-structured sir epidemic model with pulse vaccination strategy. *J. Syst. Sci. Complexity* **2012**, *25*, 417−429.

(31) Da Cruz, A. R.; Cardoso, R. T. N.; Takahashi, R. H. C. Multi-objective design with a stochastic validation of vaccination campaigns. *IFAC Proc. Vol.* **2009**, *42*, 289−294.

(32) Cordova, M. L. C.; Geletu, A.; Li, P. Optimal scheduling of vaccination campaigns using a direct dynamic optimization method. *IFAC-PapersOnLine* **2016**, *49*, 207−212.

(33) Kocis, G. R.; Grossmann, I. E. Computational experience with DICOPT solving MINLP problems in process systems engineering. *Comput. Chem. Eng.* **1989**, *13*, 307−315.

https://doi.org/10.1021/acs.iecr.1c03647
Ind. Eng. Chem. Res. 2021, 60, 17650−17662